

Can massive primordial black holes be produced in mild waterfall hybrid inflation?

Masahiro Kawasaki and Yuichiro Tada

Institute for Cosmic Ray Research, The University of Tokyo, Kashiwa, Chiba 277-8582, Japan

Kavli Institute for the Physics and Mathematics of the Universe (WPI), UTIAS, The University of Tokyo, Kashiwa, Chiba 277-8583, Japan

E-mail: kawasaki@icrr.u-tokyo.ac.jp, yuichiro.tada@ipmu.jp

Abstract. We studied the possibility whether the massive primordial black holes (PBHs) surviving today can be produced in hybrid inflation. Though it is of great interest since such PBHs can be the candidate for dark matter or seeds of the supermassive black holes in galaxies, there have not been quantitatively complete works yet because of the non-perturbative behavior around the critical point of hybrid inflation. Therefore, combining the stochastic and δN formalism, we numerically calculated the curvature perturbations in a non-perturbative way and found, without any specific assumption of the types of hybrid inflation, PBHs are rather overproduced when the waterfall phase of hybrid inflation continues so long that the PBH scale is well enlarged and the corresponding PBH mass becomes sizable enough.

Keywords: inflation, primordial black holes

ArXiv ePrint: [1512.03515](https://arxiv.org/abs/1512.03515)

Contents

1	Introduction	1
2	Aspects of hybrid inflation	2
3	Parameter search	6
3.1	Stochastic formalism	6
3.2	Mean and variance of e-folds	8
3.3	PBH abundance	10
4	Examples of power spectrum	13
5	Conclusions	14

1 Introduction

The primordial black holes (PBHs) are theoretically suggested black holes produced in the early universe. They are formed by the gravitational collapse of the Hubble patches which are $\mathcal{O}(1)$ denser than their surroundings in the radiation dominant [1–3]. The PBH abundance is connected to the properties of the primordial curvature perturbations, which determines how rare such quite overdense patches are. As an interesting point of the PBH, it is one of the well-studied candidates for dark matter (DM). While all windows for PBHs to be a main component of DM seem to be closed recently [4], there may be some loopholes. For example, the constraints for around $10^{23-24} \text{ g} \sim 10^{-10} M_{\odot}$ from neutron stars are still under discussion (see e.g. [5–8] as related works).

Another important motivation of PBHs is to explain the seeds of supermassive black holes (SMBHs). Most galaxies including our Milky Way are thought to possess one or a few SMBHs whose masses reach to $10^{6-9.5} M_{\odot}$ in their centers [9], and moreover, such massive black holes have been found even at high redshifts as $z \sim 6-7$ [10, 11]. While the astrophysical production mechanism of (especially high- z) SMBHs has still been unknown, the literature suggested massive PBHs ($\sim 10^5 M_{\odot}$) can be the seeds of SMBHs [12]. Therefore, whether sufficiently massive PBHs can be produced (*naturally* if possible) or not is an important subject.

While various mechanisms to produce massive PBHs have been proposed (*double inflation*: [13–17], *running mass*: [18, 19], *curvaton*: [20, 21], *gauge field production*: [22, 23]), we will focus on hybrid inflation in this paper. Hybrid inflation, which was originally proposed by Linde [24], is a combined model of chaotic and hilltop inflation. In this model, the inflationary universe is driven by the false vacuum energy of the so-called waterfall field, represented as ψ here, which is stabilized by the coupling to the other scalar inflaton, denoted by ϕ , at first. Then, when the inflaton’s vev becomes small due to the potential of itself and the coupling between ϕ and ψ gets to unable to stabilize the waterfall field, inflation will terminate by the second order phase transition of ψ . Hybrid inflation is an attractive model in the point that the initial condition problem is improved well in this model even though it is small field inflation (namely the scalar fields’ vev does not exceed the Planck scale).

The mainstream of hybrid inflation is models where the inflaton’s slow-roll phase (called *valley phase* generically) continues more than 60 e-folds and the waterfall transition ends instantaneously. Among this type, the original model where the inflaton’s potential is given by simple mass term predicts blue-tilted curvature perturbations which have been excluded now, but the supersymmetric flat inflaton whose potential can be raised up logarithmically due to the Coleman-Weinberg correction can give a red-tilted spectrum [25], and moreover, it has been suggested that the additional linear potential from the soft supersymmetry (SUSY) breaking can realize $n_s \sim 0.96$ [26], which is in the Planck’s sweet spot [27]. Another direction of realizations of hybrid inflation is the long-waterfall models [28–32]. In these models, ψ ’s potential is so flat that the waterfall phase continues more than 60 e-folds like hilltop inflation.

In this paper, we will concentrate on the intermediate case, namely the mild-waterfall models where the waterfall phase continues more than a few e-folds but less than 60 e-folds. An attractive point of the mild case is that very massive PBHs can be produced a lot. That is because the perturbations can grow much around the phase transition critical point due to the flatness of the (especially ψ ’s) potential and such perturbations will be inflated during the long-lasting waterfall phase. Though the massive PBH production in mild-waterfall hybrid inflation has been discussed for a long time [33–38], there is still not a quantitatively complete work because of its non-perturbative difficulty. Around the critical point, the field perturbations affect the background dynamics itself, therefore intrinsically the scalar fields cannot be treated perturbatively during the phase transition (see [39, 40] for example).

Recently, in refs. [41, 42],¹ we have proposed some non-perturbative algorithm to calculate the power spectrum of curvature perturbations in the stochastic formalism [44–50]. Especially in ref. [42], the power spectrum in mild-waterfall hybrid inflation was calculated without perturbative expansions with respect to ϕ and ψ . Following these works, we perform a wide parameter search in this paper with use of our algorithm and conclude that PBHs are rather overproduced in most of the mild-waterfall cases. Also we show the parameter constraints from the PBH constraints.

The rest of the paper is organized as follows. In section 2, we introduce hybrid inflation and briefly review the analytic approximations for the scalar dynamics and curvature perturbations, following ref. [38]. In section 3, we perform a rough parameter search and find that PBHs are overproduced in the mild-waterfall cases. Also the parameter constraints including the non-Gaussian effects are obtained as a main result of the paper. In section 4, we exemplify the power spectra of the curvature perturbations, which indicate that the allowed PBH mass scales are indeed small, with use of our algorithm. Finally section 5 is devoted to conclusions.

2 Aspects of hybrid inflation

In this section, we would like to introduce hybrid inflation and its various aspects. Throughout this paper, we do not assume any specific UV-theoretical motivation like SUSY and simply refer to the models whose potential is given by the following form as *hybrid inflation*.

$$V(\phi, \psi) = V(\phi) + \Lambda^4 \left[\left(1 - \frac{\psi^2}{M^2} \right)^2 + 2 \frac{\phi^2 \psi^2}{\phi_c^2 M^2} \right]. \quad (2.1)$$

¹Recently Vennin and Starobinsky has verified this formalism and found some analytic expressions with use of techniques of stochastic calculus [43].

Here ϕ and ψ are two real scalar field which are called *inflaton* and *waterfall* fields respectively, while Λ , M , and ϕ_c are dimensionful model parameters.² As the second term indicates, the sign of the ψ 's effective mass squared, $m_{\psi,\text{eff}}^2|_{\psi\sim 0} = \partial_\psi^2 V|_{\psi\sim 0} = 2\frac{\Lambda^4}{M^2} \left(\frac{\phi^2}{\phi_c^2} - 1\right)$, is determined by ϕ 's vev. Namely, if ϕ 's vev is larger than the critical value ϕ_c , ψ is stabilized to the origin due to its positive mass squared. Then, with the pseudo-flat $V(\phi)$ which is minimized around the origin, the inflaton can undergoes a slow roll to its minimum and *switch on* the tachyonic property of the waterfall field when ϕ reaches ϕ_c . Subsequently inflation will be ended by the second order phase transition of ψ .

The stage before ϕ reaches ϕ_c is called *valley phase* and that after ϕ_c is referred as *waterfall phase* generically. Though the waterfall phase basically ends instantaneously due to the tachyonic instability, the literatures [28–32] suggested the possibility of the long-lasting waterfall. In this paper, we concentrate on the mild-waterfall case where the waterfall phase continues more than a few e-folds but less than about 60 e-folds. That is, the phase transition occurs around the middle between the horizon exit of the scale of the cosmic microwave background (CMB) and the end of inflation. In such cases, ϕ 's vev is almost equal to ϕ_c during about 60 e-folds and therefore we can Taylor expand the inflaton's potential $V(\phi)$ around ϕ_c regardless of the motivating UV theories. Namely, adopting the notation of ref. [38], we analyze the following form of the potential.

$$V(\phi, \psi) = \Lambda^4 \left[\left(1 - \frac{\psi^2}{M^2}\right)^2 + 2\frac{\phi^2\psi^2}{\phi_c^2 M^2} + \frac{\phi - \phi_c}{\mu_1} - \frac{(\phi - \phi_c)^2}{\mu_2^2} \right]. \quad (2.2)$$

It has five dimensionful parameters as Λ , M , ϕ_c , μ_1 , and μ_2 . Among them, two d.o.f. can be fixed by the information of the amplitude and tilt of the power spectrum of the curvature perturbations on the CMB scale. In the mild-waterfall case, the CMB scale corresponds with the point in the valley phase, where the waterfall field is still irrelevant due to its large mass. Therefore the perturbations can be analyzed linearly as the simple single-field slow-roll case. At first the slow-roll parameters are given by,

$$\epsilon_V = \frac{M_p^2}{2} \left(\frac{V_\phi}{V} \right) \Big|_{\phi\sim\phi_c, \psi\sim 0} \simeq \frac{M_p^2}{2\mu_1^2}, \quad \eta_V = M_p^2 \frac{V_{\phi\phi}}{V} \Big|_{\phi\sim\phi_c, \psi\sim 0} \simeq -\frac{2M_p^2}{\mu_2^2}, \quad (2.3)$$

where M_p is the reduced Planck mass $\sqrt{8\pi G}^{-1} \simeq 2.4 \times 10^{18} \text{ GeV} \simeq 4.3 \times 10^{-6} \text{ g}$. The spectral index n_s is, in the slow-roll limit,

$$n_s = 1 - 6\epsilon_V + 2\eta_V \simeq 1 - \frac{4M_p^2}{\mu_2^2}, \quad (2.4)$$

where we assumed that η_V dominates ϵ_V (as can be checked easily for specific parameter regions shown in the following sections), which is the case for small field inflation. From this

²This potential has Z_2 symmetry as $\psi \longleftrightarrow -\psi$ which is broken at the end of inflation, and therefore it actually causes domain walls and spoils the standard cosmology. To avoid domain walls, usually one more real scalar is added as the waterfall fields and $SO(2)$ symmetry is imposed on them. It replaces domain walls with cosmic strings but they are harmless if the vev of the waterfall fields is sufficiently small. Moreover any topological defect might be avoided with much more d.o.f. for the waterfall direction. In any case, these modifications of the potential will cause only factor differences in respect of the inflationary phenomenology and we will consider this single waterfall field case for simplicity (the authors of [37] concluded that the power spectrum is suppressed by factor \mathcal{N} for the \mathcal{N} -waterfall field case).

relation, with the Planck's best fit value $n_s \simeq 0.9655$ [27], μ_2 should be fixed to,

$$\frac{\mu_2}{M_p} = \frac{2}{\sqrt{1-n_s}} \simeq 11. \quad (2.5)$$

Also the amplitude of the power spectrum is given by,

$$A_s = \frac{1}{24\pi^2 M_p^4} \frac{V}{\epsilon_V} \simeq \frac{\Lambda^4 \mu_1^2}{12\pi^2 M_p^6}. \quad (2.6)$$

Again it should be fixed by the Planck's result $A_s \simeq 2.198 \times 10^{-9}$, which gives the following relation:

$$\left(\frac{\Lambda}{M_p}\right)^4 \simeq 2.198 \times 10^{-9} \times 12\pi^2 \left(\frac{\mu_1}{M_p}\right)^{-2}. \quad (2.7)$$

In the following sections, we will fix Λ with this constraint and take M, ϕ_c and μ_1 as free parameters.

In ref. [38], Clesse and Garcia-Bellido (CG) analytically approximated the curvature perturbations during the waterfall phase and estimated the PBH abundance. At first they calculated the variance of the waterfall field at the critical point, namely $\sigma_\psi^2 = \langle \psi^2 \rangle|_{\phi=\phi_c}$, in the stochastic formalism which we will describe in the next section, as,

$$\sigma_\psi = \left(\frac{\sqrt{2}\Lambda^4 M \phi_c^{1/2} \mu_1^{1/2}}{96\pi^{3/2} M_p^4} \right)^{1/2}. \quad (2.8)$$

Then it was used as an initial condition of ψ at the beginning of the waterfall phase, that is $\psi_0 = \psi|_{\phi=\phi_c} \simeq \sigma_\psi$. The curvature perturbations were finally calculated by the standard linear perturbation theory. We briefly review the results below, while the details are omitted.

With the potential (2.2), the slow-roll e.o.m. is given by,

$$\begin{cases} 3H\dot{\phi} = -V_\phi \simeq -\frac{\Lambda^4}{\mu_1} - \frac{4\Lambda^4\psi^2}{M^2\phi_c^2}\phi, & (2.9) \\ 3H\dot{\psi} = -V_\psi \simeq -\frac{4\Lambda^4}{M^2} \left(\frac{\phi^2}{\phi_c^2} - 1 \right) \psi, & (2.10) \end{cases}$$

where V_ϕ and V_ψ denotes the derivatives of the potential with respect to ϕ and ψ . Here we omitted the higher-order terms. Then CG divided the waterfall phase into two stage; in the first phase-1 the second term of the right side of eq. (2.9) is negligible and in the phase-2 that dominates over the first term. With the approximation $H^2 \simeq \Lambda^4/3M_p^2$, the e-folds for the phase-1 and 2 can be calculated as,

$$N_1 \simeq \frac{\sqrt{\chi_2} M \phi_c^{1/2} \mu_1^{1/2}}{2M_p^2}, \quad N_2 \simeq \frac{M \phi_c^{1/2} \mu_1^{1/2}}{4M_p^2 \sqrt{\chi_2}}, \quad (2.11)$$

where,

$$\chi_2 = \log \left(\frac{\phi_c^{1/2} M}{2\mu_1^{1/2} \psi_0} \right), \quad (2.12)$$

gives the ψ 's field value at the transition point between phase-1 and 2 by $\psi = \psi_0 e^{\chi_2}$. Therefore the total e-folds for the waterfall phase is given by,

$$N_{\text{water}} \simeq N_1 + N_2 \simeq \left(\frac{\sqrt{\chi_2}}{2} + \frac{1}{4\sqrt{\chi_2}} \right) \frac{M\phi_c^{1/2}\mu_1^{1/2}}{M_p^2}. \quad (2.13)$$

Also, according to the δN formalism [51–55], the power spectrum of the curvature perturbations can, in the linear perturbation theory, be approximated by,

$$\mathcal{P}_\zeta(k) = \frac{k^3}{2\pi^2} \int d^3x \langle \zeta(0)\zeta(\mathbf{x}) \rangle e^{-i\mathbf{k}\cdot\mathbf{x}} \simeq \frac{H^2}{(2\pi)^2} (N_\phi^2 + N_\psi^2) \Big|_{aH=k}, \quad (2.14)$$

where N_ϕ and N_ψ are the derivatives of the backward e-folds with respect to ϕ and ψ respectively. Assuming the dominant contribution comes from the variation of the phase-1 e-folds N_1 due to the ψ 's fluctuations, the power spectrum is given by,

$$\mathcal{P}_\zeta(k) \simeq \frac{\Lambda^4 M^2 \phi_c \mu_1}{192\pi^2 M_p^6 \chi_2 \psi_k^2}, \quad (2.15)$$

with $\psi_k = \psi_0 e^{\chi_k}$, $\chi_k = 4\phi_c \mu_1 \xi_k^2 / M^2$, and $\xi_k = -M_p^2 (N_1 + N_2 - N_k) / (\phi_c \mu_1)$. N_k is the backward e-folds corresponding with considered comoving scale k , namely $k = e^{-N_k} k_f$ where k_f is the comoving horizon scale aH at the end of inflation. The power spectrum is maximal at the critical point as,

$$\mathcal{P}_{\zeta,\text{max}} \simeq \frac{\Lambda^4 M^2 \phi_c \mu_1}{192\pi^2 M_p^6 \chi_2 \psi_0^2} = \frac{M\phi_c^{1/2}\mu_1^{1/2}}{2\sqrt{2\pi}M_p^2\chi_2}. \quad (2.16)$$

There are two key points in these results. The first one is that the power spectrum given by CG has its maximum exactly at the critical point. However, in our calculation, the power spectrum is maximized slightly after the critical point as shown in section 4 because the quantum fluctuations of the waterfall field themselves become larger after the critical point due to its tachyonic mass.

As the second and much more important point, both of the e-folding numbers for the waterfall phase N_{water} and the maximum of the power spectrum $\mathcal{P}_{\zeta,\text{max}}$ depend almost only on the specific parameter combination $M^2\phi_c\mu_1/M_p^4$ called Π^2 by CG, except for the small logarithmic dependence due to χ_2 . Indeed, from eqs. (2.13) and (2.16), we can easily find a one-to-one monotonic increase correspondence between N_{water} and \mathcal{P}_ζ . Before that, let us clarify the typical value of χ_2 . Substituting the initial condition $\psi_0 = \sigma_\psi$ (2.8) into eq. (2.12) and using the CMB normalization (2.7),³ χ_2 can be simply written as,

$$\chi_2 = \log \left(\left(\frac{2}{\pi} \right)^{1/4} A_s^{-1/2} \Pi^{1/2} \right), \quad \Pi^2 = \frac{M^2\phi_c\mu_1}{M_p^4}, \quad (2.17)$$

where $A_s = 2.198 \times 10^{-9}$. From this expression, it can be seen that χ_2 is around 10 for typical values $10 \lesssim \Pi^2 \lesssim 1000$ in the mild-waterfall cases. Therefore, from eqs. (2.13) and (2.16), we can obtain the following relation, which does not depend on any detail parameterization.

$$\mathcal{P}_{\zeta,\text{max}} \simeq \frac{1}{\sqrt{2\pi}\chi_2^3} N_{\text{water}} \simeq 0.01 N_{\text{water}}. \quad (2.18)$$

³ Even if we do not use the CMB normalization and deal with Λ as a free parameter, χ_2 depends on Λ only logarithmically.

Here we neglected the $\chi_2^{-1/2}$ term in eq. (2.13). Since the PBH constraints on the curvature perturbations are $\mathcal{P}_\zeta \lesssim \mathcal{O}(0.01)$ as we will mention in the next section, it can be obviously seen that the PBH overproduction is inevitable in the mild-waterfall cases such that $N_{\text{water}} \gtrsim \mathcal{O}(10)$. In the next section, we will check and clarify this estimation with use of the stochastic formalism.

3 Parameter search

Though we reviewed the result in the linear perturbation theory in the previous section, the dynamics of the waterfall field around the critical point is actually dominated by the Hubble fluctuations. Therefore the linear perturbation with respect to ψ around the critical point essentially breaks down (c.f. [39, 40]). Accordingly we calculate the curvature perturbations without the perturbative expansions with respect to ϕ and ψ with use of the stochastic formalism. In this section we introduce the stochastic formalism at first. Then we calculate the curvature perturbations in the wide parameter region. From their results, we conclude that PBHs are overproduced in the mild-waterfall cases as a main claim of this paper.

3.1 Stochastic formalism

The stochastic formalism was proposed by Starobinsky in 1986 [44] (see also [45–50]). In this formalism, the superhorizon coarse-grained fields, namely,

$$\phi_{\text{IR}}(t, \mathbf{x}) = \int \frac{d^3k}{(2\pi)^3} W\left(\frac{k}{\epsilon aH}\right) e^{i\mathbf{k}\cdot\mathbf{x}} \phi_{\mathbf{k}}(t), \quad (3.1)$$

are treated as the classical background fields. Here $W(k/k_s)$ is a window function and ϵ is a small positive parameter. As a window function, the simple step function $\theta(\epsilon aH - k)$ is often used for brevity. ϵ divides the scalar fields into the classicalized part and the quantum part. That is, the modes for $k < \epsilon aH$ are well classicalized and can be treated as classical fields, while the modes for $k > \epsilon aH$ should be assumed to be the quantum operators. To take sufficiently superhorizon modes and also validate the perturbative expansions with respect to ϵ which we use below, ϵ should be less than unity. In this paper the value of 0.01 is mainly used for ϵ , while several results for $\epsilon = 0.1$ are also shown to see the ϵ -dependences.

For the above coarse-grained fields, the e.o.m. reads [56],

$$\begin{cases} \frac{d\phi_{\text{IR},i}}{dN} = \frac{\pi_{\text{IR},i}}{H} + \mathcal{P}_{\phi_i}^{1/2}(k = \epsilon aH)\xi_i, \\ \frac{d\pi_{\text{IR},i}}{dN} = -3\pi_{\text{IR},i} - \frac{V_i}{H}, \end{cases} \quad (3.2)$$

in the leading order with respect to ϵ . $\mathcal{P}_{\phi_i}^{1/2}$ denotes the power spectrum of ϕ_i , i.e. $\mathcal{P}_{\phi_i}(k) = \frac{k^3}{2\pi^2} \int d^3x \langle \phi_i(0)\phi_i(\mathbf{x}) \rangle e^{-i\mathbf{k}\cdot\mathbf{x}}$. The subscript i labels the flavors of the scalar fields for the multi-field cases. Without the term of ξ_i , it is recovered to the standard e.o.m. for the homogenous fields. This ξ term as an important difference is interpreted as a classical Gaussian

random variable having following stochastic properties.⁴

$$\begin{cases} \langle \xi_i(N, \mathbf{x}) \rangle = 0, \\ \langle \xi_i(N, \mathbf{x}) \xi_j(N', \mathbf{x}') \rangle = \delta_{ij} \frac{\sin(\epsilon a H r)}{\epsilon a H r} \delta(N - N'), \quad r = |\mathbf{x} - \mathbf{x}'|. \end{cases} \quad (3.3)$$

For the coarse-grained fields, $\frac{\sin(\epsilon a H r)}{\epsilon a H r}$ can be approximated by $\theta(1 - \epsilon a H r)$. The delta function type property for the time variable comes from the fact that we used the sharp window function for eq. (3.1). Anyway it represents the fact that *the superhorizon coarse-grained fields receive the Gaussian white noise independent for each Hubble patch and its amplitude is given by the scalar fields' perturbations $\mathcal{P}_{\phi_i}^{1/2}$* . This noise term comes from the inflow of the UV part $\phi_{UV} = \phi - \phi_{IR}$ into the IR part for every time. As we indicated, the UV part originally behaves as a quantum field but it is redshifted and classicalized at the time of $k = \epsilon a H$ to join in the IR part. At this time the exact field value of this joining mode cannot be determined due to its quantum property. Instead it is interpreted as a classical random variable and its amplitude can be calculated in quantum field theory as \mathcal{P}_{ϕ_i} of course.

Due to the noise term, every Hubble patch is assumed to evolve independently in the stochastic formalism. In this sense, the all background parameter values in eq. (3.2), namely H , V_i , and \mathcal{P}_{ϕ_i} , should be determined in each Hubble patch by the scalar field values of that patch. Inversely, if one concentrate on the dynamics of one Hubble patch, the e.o.m. reduces to the following self-closed Langevin equations.

$$\begin{cases} \frac{d\phi_i}{dN}(N) = \frac{\pi_i}{H}(N) + \mathcal{P}_{\phi_i}^{1/2}(N)\xi_i(N), \\ \frac{d\pi_i}{dN}(N) = -3\pi_i(N) - \frac{V_i}{H}(N), \\ V_i(N) = V_i(\phi_1(N), \phi_2(N), \dots), \\ 3M_p^2 H^2(N) = \sum_i \frac{\pi_i^2}{2} + V(\phi_1(N), \phi_2(N), \dots), \\ \langle \xi_i(N) \rangle = 0, \\ \langle \xi_i(N) \xi_j(N') \rangle = \delta_{ij} \delta(N - N'). \end{cases} \quad (3.4)$$

However in regards to \mathcal{P}_{ϕ_i} , one should calculate the dynamics of all subhorizon modes with the above Langevin eq. to obtain the value of them, strictly speaking. In this paper we approximate them by the constant mass solution as,

$$\mathcal{P}_{\phi_i}(k = \epsilon a H) = \frac{H^2}{8\pi} \epsilon^3 |H_{\nu_i}^{(1)}(\epsilon)|^2, \quad (3.5)$$

where $H_{\nu}^{(1)}(x)$ is the Hankel function of the first kind given by,

$$H_{\nu}^{(1)}(x) = J_{\nu}(x) + iY_{\nu}(x), \quad (3.6)$$

with the Bessel functions of the first and second kind, $J_{\nu}(x)$ and $Y_{\nu}(x)$, and ν_i is defined by,

$$\nu_i = \sqrt{\frac{9}{4} - \frac{V_{ii}}{H^2}}, \quad (3.7)$$

⁴Here we assume there is no correlation between the different flavors of ξ . However the correlations between them due to the interactions before the horizon exit can be also included. In this paper, we omit them for simplicity after easily checked that they do not affect the result at all.

for $\frac{V_{ij}}{H^2} \leq \frac{9}{4}$. For massive fields as $\frac{V_{ij}}{H^2} > \frac{9}{4}$, we simply assume that their Hubble noise vanishes. Since numerical calculations of the Bessel functions are time consuming, we use the asymptotic forms of them for small arguments as,

$$J_\nu(x) \simeq \frac{1}{\Gamma(\nu+1)} \left(\frac{x}{2}\right)^\nu, \quad Y_\nu(x) \simeq -\frac{\Gamma(\nu)}{\pi} \left(\frac{2}{x}\right)^\nu. \quad (3.8)$$

In the following sections, we numerically solve these equations simultaneously.

3.2 Mean and variance of e-folds

As we saw in the previous section, the stochastic formalism gives the e.o.m. for the scalar fields coarse-grained on the horizon scale. Therefore the dynamics of one spatial point in the stochastic formalism can be regarded as that of one Hubble patch. Namely, in the stochastic formalism, the scalar field in each Hubble patch behaves as a Brownian motion drifted by the potential force. On the other hand, according to the δN formalism [51–55], the gauge invariant curvature perturbations on the superhorizon scale are given by the difference of the e-folds between the initial flat slice and the final uniform density slice. That is, since the dynamics of each Hubble patch automatically fluctuates due to the noise, the e-folding numbers also vary over the universe and their fluctuations are nothing but the curvature perturbations. Strictly speaking, the obtained curvature perturbations are coarse-grained values on the horizon scale at the end of inflation.

Let us describe the method more concretely. At first, one must determine the initial flat slice in the valley phase and the final uniform density slice around the end of inflation. Here, regarding the initial flat slice, note that in the valley phase inflation can be approximated as the single-field case and moreover the curvature perturbations are much smaller than those expected in the waterfall phase. Therefore, neglecting the curvature perturbations, the initial flat slice can be approximated by the uniform ϕ slice and the ψ 's field value is almost irrelevant. Next, making many realizations of the Langevin equations from the initial field values to the final energy density value, one can obtain various realizations of the e-folding numbers. Their deviations from the mean value $\langle N \rangle$ are nothing but the data set of the coarse-grained curvature perturbations. Though the information of the correlation function like $\langle \zeta(\mathbf{x}_1)\zeta(\mathbf{x}_2) \rangle$ for $\mathbf{x}_1 \neq \mathbf{x}_2$ cannot be derived at this time, at least the probability distribution function (PDF) of the coarse-grained curvature perturbations can be obtained up to the realization errors. With use of this PDF, one can calculate the formation rate of PBHs whose masses are larger than that corresponding with the horizon scale at the end of inflation. In this section, let us roughly estimate the PBH abundance by this quantity and find the parameter constraints.

For parameter search, we used the following three searching regions.

$$\begin{aligned} &\bullet 10^{-4}M_p \leq M \leq 10^{-1}M_p, \quad \phi_c = \sqrt{2}M, \quad (\text{SUSY like assumption}) \\ &\bullet M = 0.1M_p, \quad 10^{-4}M_p \leq \phi_c \leq 10^{-1}M_p, \\ &\bullet 10^{-4}M_p \leq M \leq 10^{-1}M_p, \quad \phi_c = 0.1M_p. \end{aligned} \quad (3.9)$$

μ_1 is also varied so that $\Pi^2 = M^2\phi_c\mu_1/M_p^4$ takes the value up to 300. Λ is given by eq. (2.7) for each value of μ_1 . In figure 1, we plot the mean e-folds for the waterfall phase $\langle N \rangle_{\text{water}}$ and the variance of their perturbations $\langle \delta N^2 \rangle = \langle N^2 \rangle - \langle N \rangle^2$ vs. $\Pi^2 = M^2\phi_c\mu_1/M_p^4$ for various parameters in the above searching region. μ_1 is varied for each parameter set (M, ϕ_c) . Also

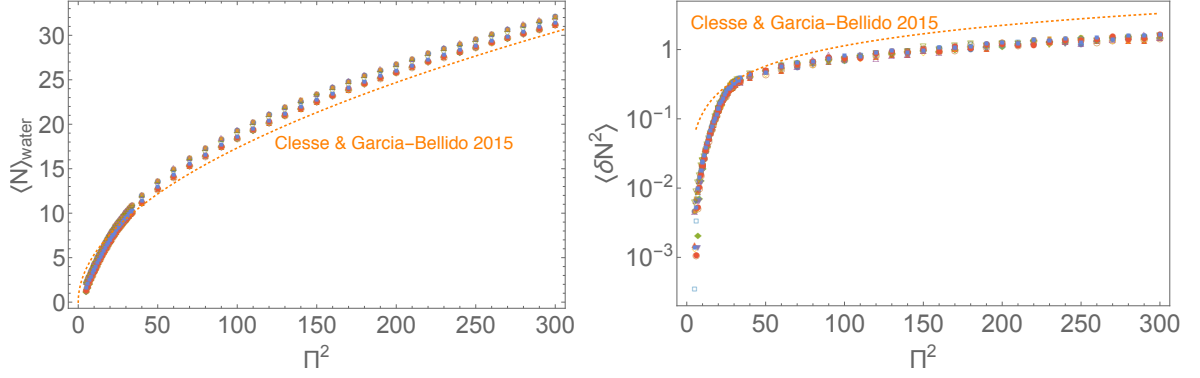


Figure 1. The mean e-folds of the waterfall phase (left panel) and the variance of their perturbations (right panel) vs. $\Pi^2 = M^2 \phi_c \mu_1 / M_p^4$ for various parameter sets in the searching region (3.9). μ_1 is varied for each set of M and ϕ_c . There are 12 sets of (M, ϕ_c) represented by different markers although they cannot be distinguished in the figure. 2000 realizations are made for each data point. It is clearly shown that both of $\langle N \rangle$ and $\langle \delta N^2 \rangle$ depend almost only on Π^2 as ref. [38] suggested. However, while their results which are represented by orange dotted lines are well consistent with our calculations for $\langle N \rangle$, there are factor differences in $\langle \delta N^2 \rangle$. Anyway these plots indicate Π^2 should be less than about 10 to satisfy the PBH constraint $\langle \delta N^2 \rangle \lesssim 0.01$ and it means the waterfall phase cannot continue more than about 5 e-folds.

the CG's analytic results (2.13) and (2.15) are shown as orange dotted lines. Here note that the variance and the power spectrum are related by,

$$\langle \delta N^2 \rangle \simeq \int_0^{\langle N \rangle_{\text{water}}} \mathcal{P}_\zeta(k) dN_k. \quad (3.10)$$

From this figure, it is found that the mean e-folds $\langle N \rangle$ obtained in the stochastic formalism is well fitted by the CG's result. On the other hand, there are factor differences in the variance $\langle \delta N^2 \rangle$. It clearly shows the non-perturbative effects which CG did not include. However at least it can be said that the full result of $\langle \delta N^2 \rangle$ also depends only on the specific parameter combination $\Pi^2 = M^2 \phi_c \mu_1 / M_p^4$. Having in mind that the variance of the curvature perturbations should be roughly less than 10^{-2} at most not to overproduce PBHs as we will show in the next subsection, it can be seen that Π^2 should be less than around 10, which indicates the waterfall phase cannot continue more than about 5 e-folds.

Here let us mention the ϵ -dependence of the results. As we said, the stochastic formalism has an indeterminate parameter ϵ which fixes the separation between the classical superhorizon and the quantum subhorizon modes. Since this is just the uncertainty of the formalism, any result should have little ϵ -dependence for reliable calculations. To see the ϵ -dependence, we also show $\langle N \rangle$ and $\langle \delta N^2 \rangle$ for $\epsilon = 0.1$ in figure 2, comparing them to those for $\epsilon = 0.01$. It shows that $\langle \delta N^2 \rangle$ has relatively large differences in low Π^2 . For low Π^2 , the waterfall phase does not continue so long as already shown. On the other hand, for small ϵ , the modes shorter than the coarse-graining scale $k = \epsilon a H$ are erased in the stochastic formalism. Specifically, since $-\log 0.01 \simeq 4.6$, the perturbations generated in about last 4.6 e-folds cannot be treated in the calculations where $\epsilon = 0.01$. Therefore, for low Π^2 , the contribution of the perturbations after the critical point cannot be taken into account well in the case of small ϵ , and that is the reason why $\langle \delta N^2 \rangle$ for $\epsilon = 0.01$ is suppressed compared to that for $\epsilon = 0.1$. Anyway the case of low Π^2 is slightly out of the range of application of the

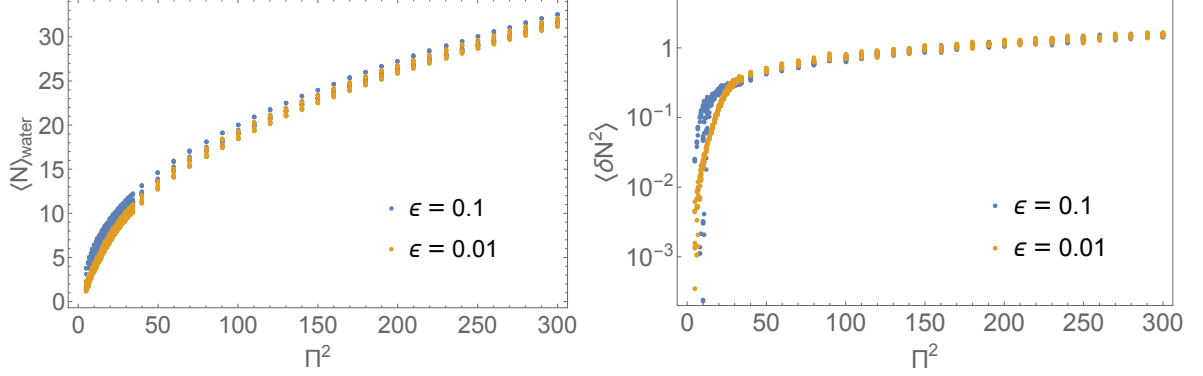


Figure 2. The same plots to figure 1 for $\epsilon = 0.1$ and 0.01 . The orange datas are the same ones of figure 1. While $\langle N \rangle_{\text{water}}$ has good agreement between different ϵ , $\langle \delta N^2 \rangle$ shows a large ϵ -dependence in low Π^2 which indicates that the results in the stochastic formalism for low Π^2 might be unreliable.

stochastic formalism, but it does not change the results for large Π^2 and the main conclusion that massive PBHs are overproduced.

3.3 PBH abundance

In this subsection, we estimate the PBH abundance including the non-Gaussian (NG) effects. Following the Press-Schechter approach [57], if the coarse-grained curvature perturbations ζ_s follow the PDF $P(\zeta_s)$, the formation rate of PBHs which are more massive than the mass corresponding with the coarse-graining scale is given by,

$$\beta(> M_{\text{PBH}}) = 2 \int_{\zeta_c}^{\infty} P(\zeta_s) d\zeta_s, \quad (3.11)$$

where ζ_c is the threshold for the PBH formation. The factor 2 is conventional to include the effects of mergers and accretions. For the case of PBHs, the mass M_{PBH} is related to the coarse-graining comoving scale R_s by,⁵

$$M_{\text{PBH}} \simeq \frac{M_p^2}{H_{\text{inf}}} (k_f R_s)^2 \simeq \frac{M_p^2}{H_{\text{inf}}} e^{2N_s} = 1.0 \times 10^4 \text{ g} \left(\frac{H_{\text{inf}}}{10^9 \text{ GeV}} \right)^{-1} e^{2N_s}. \quad (3.13)$$

Here H_{inf} is the Hubble parameter at the end of inflation and N_s denotes the corresponding backward e-folds, $R_s^{-1} = k_f e^{-N_s}$. We assumed that reheating occurs soon after inflation. If the power spectrum has a large peak which will be validated in the next section, PBHs are formed almost only on the peak scale and the above β with the coarse-graining scale being the peak scale can be directly used to be constrained.

⁵ Here we approximate the PBH mass simply by the horizon mass M_H , but it is known to scale, depending on the value of the density perturbation δ , as,

$$M_{\text{PBH}} = k M_H (\delta - \delta_c)^\gamma, \quad (3.12)$$

where δ_c represents the critical threshold value for δ , and k and γ are some numerical factors [58–60]. However this effect basically shifts the PBH mass to smaller one and therefore it will not change our main result that massive PBHs cannot be produced with the appropriate abundance in the mild-waterfall hybrid inflation.

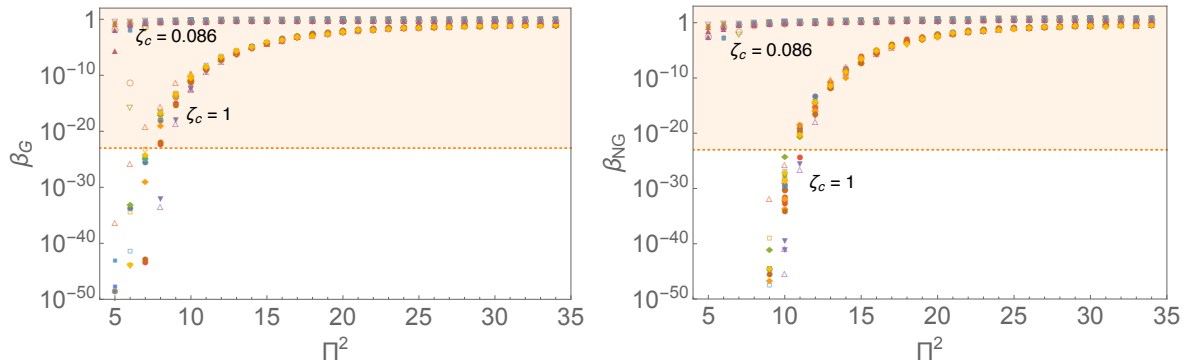


Figure 3. Left panel: the plot of the PBH abundance in the Gaussian assumption β_G (3.14) with use of the variance shown in figure 1. Namely it includes all contributions of PBHs more massive than the smallest mass scale M_p^2/H_{inf} which corresponds with the scale at the end of inflation. The bottom group is for $\zeta_c = 1$ while the upper group is for $\zeta_c \simeq 0.086$ [62]. Also the orange dotted line represents the typical constraints for light PBHs ($\lesssim 10^{15}$ g), namely $\beta \lesssim 10^{-23}$. If $\zeta_c \simeq 0.086$, there is no appropriate value of Π^2 with which PBHs are not overproduced. On the other hand, if $\zeta_c = 1$, the PBH constraints indicate $\Pi^2 \lesssim 8$, which means the waterfall phase can continue few e-folds as shown in figure 1. Right panel: the same plot with NG corrections (3.16). Though the results for $\zeta_c \simeq 0.086$ are hardly different, the PBH abundance for $\zeta_c = 1$ is suppressed for low Π^2 compared to the value without NG corrections. Then the constraints are slightly weakened to $\Pi^2 \lesssim 11$ but the duration of the waterfall phase is still as short as 4–5 e-folds.

If one assumes the curvature perturbations follow the Gaussian distribution, β can be easily estimated by,⁶

$$\beta_G = 2 \int_{\zeta_c} \frac{1}{\sqrt{2\pi\sigma_s^2}} e^{-\zeta_s^2/2\sigma_s^2} d\zeta_s, \quad (3.14)$$

where σ_s^2 denotes the variance of the coarse-grained curvature perturbations, namely, with use of some window function $W(kR_s)$,

$$\sigma_s^2 = \langle \zeta_s^2 \rangle = \int W^2(kR_s) \mathcal{P}_\zeta(k) d \log k. \quad (3.15)$$

On the left panel of figure 3, we plot the β_G with use of $\langle \delta N^2 \rangle$ shown in figure 1 as σ_s^2 for different two threshold values, that is, the simple assumption $\zeta_c = 1$ and the recent analytic prediction by Harada et al [62], $\zeta_c = \frac{1}{3} \log \frac{3(\chi_a - \sin \chi_a \cos \chi_a)}{2 \sin^3 \chi_a} \Big|_{\chi_a = \pi\sqrt{\omega}/(1+3\omega)} \simeq 0.086$ where ω is the e.o.s. for radiation, $p/\rho = 1/3$. Also we show the typical constraints for light PBHs $\beta_G \sim 10^{-23}$ as an indicator [63].⁷ Incidentally this value corresponds with 10 sigma rarity,

⁶Though we used the variance of the coarse-grained curvature perturbations here, the authors of [61] claimed that the power spectrum on the considered scale should be used instead of the variance. That is because the curvature perturbations are undamped quantities even on superhorizon scales and therefore the variance includes the much superhorizon modes, which should not affect the PBH formation. However now the power spectrum has a large peak as we will show in the next section, and the larger scale modes than the peak scale are already suppressed. Therefore using the variance will not overestimate the PBH abundance so much. Since we would like to include the NG effects by the form of the third and fourth moment, namely $\langle \delta N_s^3 \rangle$ and $\langle \delta N_s^4 \rangle$, we used the variance $\langle \delta N_s^2 \rangle$ instead of the power spectrum.

⁷Though we want massive PBHs $\gtrsim 10^{15}$ g, we will find such massive ones cannot be produced with proper abundance in hybrid inflation and then we used the constraints for light PBHs $\lesssim 10^{15}$ g.

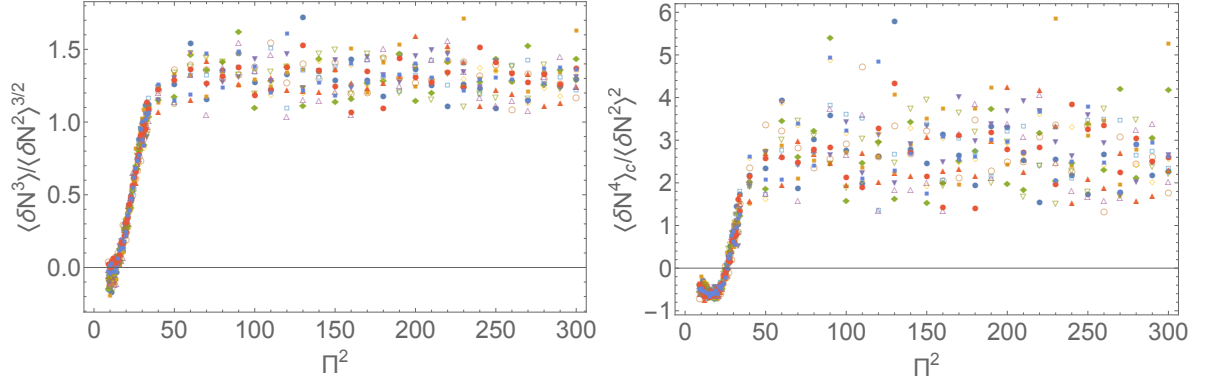


Figure 4. The skewness $S^{(3)} = \langle \delta N^3 \rangle / \langle \delta N^2 \rangle^{3/2}$ and kurtosis $S^{(4)} = \langle \delta N^4 \rangle_c / \langle \delta N^2 \rangle^2$ where $\langle \delta N^4 \rangle_c = \langle \delta N^4 \rangle - 3 \langle \delta N^2 \rangle^2$ is a connected part of the fourth moment. It clearly indicates the non-negligible $\mathcal{O}(1)$ NG.

i.e. $\zeta_c \sim 10\sigma_s$. Therefore this constraint roughly indicates $\mathcal{P}_\zeta \sim \sigma_s^2 \lesssim 0.01$ for $\zeta_c = 1$ as mentioned previously. The figure shows Π^2 should be less than around 8 for the case $\zeta_c = 1$, which means the waterfall phase can continue few e-folds. Also there is almost no proper parameter set with which PBHs are not overproduced if $\zeta_c \simeq 0.086$.

On the other hand, the curvature perturbations produced around the critical point are naively thought to have NG as indicated by its non-perturbativity. In figure 4, we show the skewness $S^{(3)} = \langle \delta N^3 \rangle / \langle \delta N^2 \rangle^{3/2}$ and kurtosis $S^{(4)} = \langle \delta N^4 \rangle_c / \langle \delta N^2 \rangle^2$ where $\langle \delta N^4 \rangle_c = \langle \delta N^4 \rangle - 3 \langle \delta N^2 \rangle^2$ is a connected part of the fourth moment. These values vanish in a pure Gaussian case, so non-zero values of them directly indicate the NG of the curvature perturbations. As we predicted, these plots show non-negligible $\mathcal{O}(1)$ NG.⁸

These NG modifies the PDF of the curvature perturbations and then β is given by,

$$\begin{aligned} \beta_{\text{NG}} &\simeq \frac{2}{\sqrt{2\pi}} \int_\nu^\infty d\alpha \exp \left[\sum_{n=3}^4 \frac{(-1)^n}{n!} S^{(n)} \frac{\partial^n}{\partial \alpha^n} \right] \exp \left[-\frac{\alpha^2}{2} \right] \\ &\simeq \sqrt{\frac{2}{\pi}} \frac{1}{\nu} \exp \left[\sum_{n=3}^4 \frac{\nu^2}{n!} S^{(n)} \right] e^{-\nu^2/2}, \end{aligned} \quad (3.16)$$

where ν is defined by $\nu = \zeta_c / \sigma_s$ and we used the high peak limit $\nu \gg 1$ in the second line. Though we truncated them here, it is possible to include the higher order terms than fourth order (see also appendix K of ref. [64]). This modified probability is plotted on the right panel in figure 3. Compared to the Gaussian case (left panel), it can be seen that the probability for small Π^2 is suppressed for $\zeta_c = 1$, while the result for $\zeta_c = 0.086$ hardly changes. As a result, the constraint for Π^2 in the $\zeta_c = 1$ case is weakened to $\Pi^2 \lesssim 11$, which corresponds with $\langle N \rangle_{\text{water}} \lesssim 4$.

Let us briefly summarize the above results here. We calculated e-folds numerically in the stochastic formalism and checked that the mean e-folds for the waterfall phase and their variance depend almost only on some specific parameter combination $\Pi^2 = M^2 \phi_c \mu_1 / M_p^4$.

⁸However the NG is not as large as has been considered. Refs. [34, 35] concluded the curvature perturbations have a negative chi-squared type distribution, namely $\zeta(\mathbf{x}) = -(g^2(\mathbf{x}) - \langle g^2 \rangle)$, where g is a Gaussian field. But this distribution type gives $S^{(3)} = -2\sqrt{2}$ and $S^{(4)} = 12$ which are larger enough than our result. Therefore our calculations give less NG curvature perturbations than the simple chi-squared ansatz.

However simultaneously it was found that the variance of the perturbations becomes large for mild-waterfall hybrid inflation. In fact, if $\zeta_c = 0.086$ [62], there is no parameter region where PBHs are not overproduced. Only if the PBH mass given by eq. (3.13) is lighter than 10^9 g, the constraint can be avoided because such PBHs are evaporated before big-bang nucleosynthesis (BBN). On the other hand, if the threshold is as high as $\zeta_c = 1$, the PBH overproduction roughly gives the parameter constraint as $\Pi^2 \lesssim 8$ (or 11 with NG corrections) which means the waterfall phase can continue few e-folds. It is too short to produce PBHs massive enough to be DMs or seeds of SMBHs. This is the main result of this paper.

Here note that the coarse-graining scale is the Hubble scale at the end of inflation, which is the smallest scale, and therefore β shown in this section includes all contributions of various mass PBHs. However, as we will see in the next section, the power spectrum has large and only one peak and therefore the main contribution for β is given almost only by the PBHs whose mass corresponds with the peak scale. Hence the resulting β for peak scale can be approximated well by that obtained in this section.

4 Examples of power spectrum

In the previous section, we estimated the PBH abundances with use of the curvature perturbations coarse-grained on the Hubble scale at the end of inflation. For them to be a good approximation, it is needed that the power spectrum has only one large peak. Moreover it is still unknown where the peak scale is. To clarify them, in this section we show some examples of the power spectra calculated in the stochastic- δN algorithm [41, 42].

Let us briefly review the algorithm at first. As mentioned repeatedly, in the stochastic formalism the dynamics in each Hubble patch is treated as an individual Brownian motion drifted by the potential force. The correlative information for two distant points is imprinted in the time when those two points are separated farther than the horizon scale. That is, while the scalar fields on two points evolves conjointly before the horizon exit, they start moving individually due to the non-correlating noise after their distance is larger than the Hubble size. It means the perturbations of the e-folding numbers obtained for the paths branching from one field-phase-space point include only the modes which exit the horizon between the branching time and the end of inflation. Thus the following relation is satisfied.

$$\langle \delta N^2 \rangle = \int_{\log k_f - \langle N \rangle}^{\log k_f} \mathcal{P}_\zeta d \log k, \quad (4.1)$$

where $\langle N \rangle$ is the mean e-folding number from the branching point to the end of inflation. Inversely the power spectrum can be obtained from changing the branching point slightly as,

$$\mathcal{P}_\zeta(k) = \left. \frac{d}{d \langle N \rangle} \langle \delta N^2 \rangle \right|_{\langle N \rangle = \log(k_f/k)}. \quad (4.2)$$

Here note that k_f represents rather $\epsilon aH|_f$ than $aH|_f$.

While the branching point vev and the mean e-folds have a one-to-one correspondence in the single-field slow-roll case, there is only the uniform mean e-folds hypersurface on the field phase space in the multi-field case. Therefore the branching points should be properly weighted by the realization probability, which is reproduced by making various sample paths. Concretely, we use the following algorithm.

1. Determine the initial field value from which the mean e-folds is about 60. It represents the field value of our observable universe at 60 e-folds before the end of inflation.⁹
2. Make one sample path by integrating the Langevin eqs. (3.4) and (3.5) from the initial field value. It shows the dynamics of some Hubble patch in our observable universe.
3. Produce various realizations branching from some point on the produced sample path and calculate the e-folds for them to the final uniform density surface around the end of inflation. They give the mean and variance of the e-folds, referred as $\langle N_1 \rangle$ and $\langle \delta N_1^2 \rangle$ here.
4. Repeat the procedure 3 with slightly different branching point on the same sample path to obtain another set of the mean and variance $\langle N_2 \rangle$ and $\langle \delta N_2^2 \rangle$. Then the power spectrum on the scale $k \simeq k_f e^{-\langle N_1 \rangle + \langle N_2 \rangle / 2}$ can be approximated by,

$$\mathcal{P}_\zeta(k) \simeq \frac{\langle \delta N_1^2 \rangle - \langle \delta N_2^2 \rangle}{\langle N_1 \rangle - \langle N_2 \rangle}. \quad (4.3)$$

This power spectrum is obtained from the paths branching from one sample path. Therefore this result is valid only in the region spatially near to that sample path.

5. To obtain the power spectrum valid over our universe, iterate the procedure 2–4 and average the obtained power spectra. This averaged one represents the true power spectrum obtained in our observable universe.

With use of the above algorithm, we calculate the power spectrum for $\Pi^2 = 10, 30$, and 50, and the results are shown in figure 5, compared to those for $\epsilon = 0.1$ and the CG's analytic approximations. While they are not so different for $\Pi^2 = 30$ or 50, the peak for $\epsilon = 0.01$ is much smaller than that for $\epsilon = 0.1$ or the CG's one for $\Pi^2 = 10$. This is simply because $-\log 0.01 \simeq 4.61$ is larger than the peak scale $N_{\text{peak}} \sim 4$. Namely the peak scale is smaller than $(\epsilon a H|_f)^{-1}$ for $\epsilon = 0.01$, which is the smallest scale the stochastic formalism can treat. Therefore the result for low Π^2 around 10 may be unreliable, but anyway the corresponding PBH mass $M_{\text{PBH}} \sim \frac{M_p^2}{H_{\text{inf}}} e^{2 \times 4} = 3.0 \times 10^7 \text{ g} \left(\frac{H_{\text{inf}}}{10^9 \text{ GeV}} \right)^{-1}$ is still too small and our main conclusion that massive PBHs are overproduced in hybrid inflation is not changed.

5 Conclusions

In this paper we study the possibility whether massive PBHs can be produced in mild-waterfall hybrid inflation whose potential can be parametrized as eq. (2.2). As a recent related work, Clesse and Garcia-Bellido (CG) [38] estimated the curvature perturbations during the waterfall phase in the linear δN formalism and found that the results depend almost only on the specific parameter combination $\Pi^2 = M^2 \phi_c \mu_1 / M_p^4$ as briefly reviewed in section 2. However, since the waterfall field dynamics is dominated by the Hubble fluctuations around the critical point, one must go beyond the linear perturbation theory to calculate

⁹The power spectrum obtained by the following procedure depends on this initial field value in principle. This ambiguity is not only for our algorithm. The predictability of the inflation model generically reduces unless the inflatons' trajectory converge well at least on the CMB scale. In our hybrid inflation case, the CMB scale mode exits the horizon in the well-converging valley phase, and indeed the result is not affected by the initial condition so much.

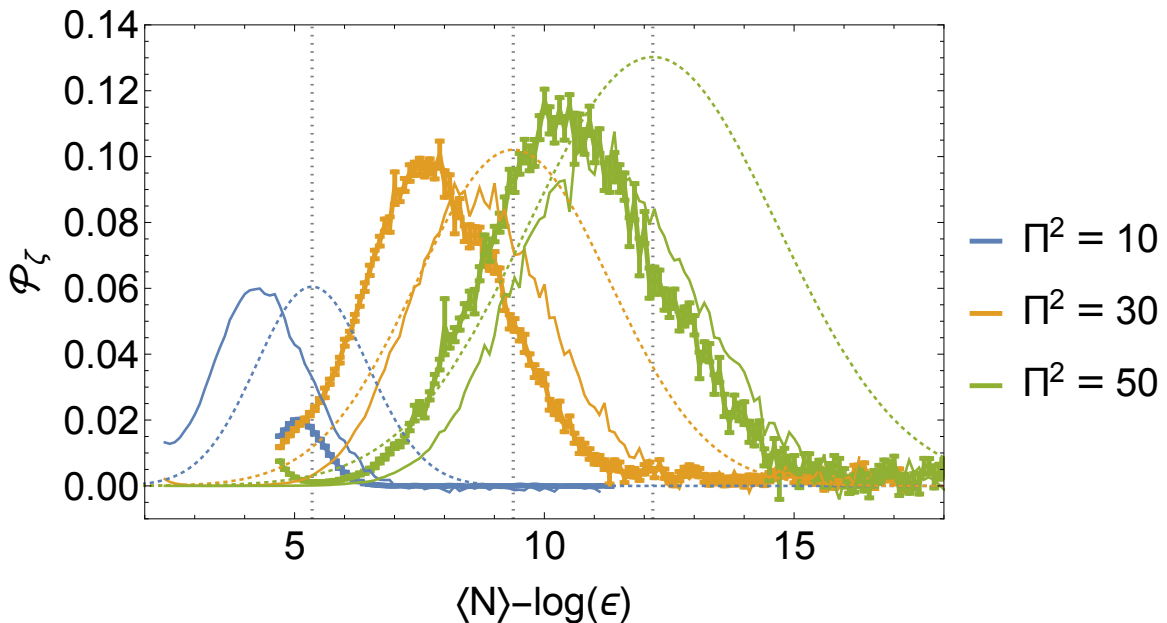


Figure 5. The power spectrum calculated in the stochastic- δN algorithm [41, 42]. The thick lines with error bars represent the results for $\epsilon = 0.01$, while the plane and dotted lines denote those for $\epsilon = 0.1$ and the CG's analytic approximations respectively. For $\epsilon = 0.1$, we omit the error bars to avoid a busy figure. The color variation represents the difference of Π^2 , but M and ϕ_c are fixed to $0.1M_p$ and $0.1\sqrt{2}M_p$ respectively. Each power spectrum is averaged over 2500 sample paths and on each data point 1000 paths are made for each sample path. The error bars represent the standard errors. The horizontal axis shows the corresponding scale including $-\log \epsilon$ to cancel the scale shift due to the variation of ϵ . From left to right, the vertical gray dotted lines represent the times when the paths pass the critical point for $\Pi^2 = 10, 30$, and 50 . It suggests that the power spectrum has a peak slightly after the critical point, which reflects that the ψ 's noise itself becomes slightly large after the critical point due to its tachyonic mass.

the curvature perturbations. Accordingly we calculate the curvature perturbations without perturbative expansions with respect to the scalar fields, combining the stochastic and δN formalism.

In section 3, the variance of the curvature perturbations is calculated for various parameter values as shown in figure 1, and it shows that indeed the curvature perturbations depend almost only on Π^2 though there are factor differences between our and CG's result. Subsequently we estimate the PBH abundance with use of this variance including the non-Gaussian effect as plotted in figure 3. The abundance is calculated both for the simple assumption of the threshold, namely $\zeta_c = 1$, and the recent analytic work $\zeta_c \simeq 0.086$ [62]. As a result, the specific parameter combination $\Pi^2 = M^2\phi_c\mu_1/M_p^4$ should be less than around 11 not to overproduce PBHs if $\zeta_c = 1$, which means that the waterfall phase can continue only 4–5 e-folds at most. Also, if $\zeta_c \simeq 0.086$, Π^2 should be smaller than ~ 1 . In section 4, we show some examples of the power spectra calculated in the stochastic- δN formalism [41]. They indicate that the power spectrum has one large peak slightly after the critical point.

In summary, the specific parameter combination $\Pi^2 = M^2\phi_c\mu_1/M_p^4$ should be less than around 11 for $\zeta_c = 1$ and then the waterfall phase cannot continue so long. Moreover in such cases the power spectrum shows a peak near the end of inflation $N_{\text{peak}} \lesssim 4$ and therefore the

corresponding PBH mass scale is given by $M_{\text{PBH}} \lesssim \frac{M_p^2}{H_{\text{inf}}} e^{2 \times 4} = 3.0 \times 10^7 \text{ g} \left(\frac{H_{\text{inf}}}{10^9 \text{ GeV}} \right)^{-1}$. It is much smaller than the desired one (comparable to $M_{\odot} \sim 10^{33} \text{ g}$) because the corresponding scale does not benefit by the exponential inflating during the waterfall phase so much.

As briefly mentioned in footnote 2, ref. [37] claimed that the power spectrum can be suppressed by the factor \mathcal{N} with \mathcal{N} -waterfall fields. Therefore, if there are about 100 waterfall fields and a continuous symmetry is imposed on them, one can obtain the desirable amplitude of the perturbations as $\langle \delta N^2 \rangle \sim 0.01$ even for large Π^2 . To verify such a dependence of the power spectrum on the number of the waterfall fields in a non-perturbative way, we should apply the stochastic- δN formalism for the multi-waterfall cases. It is beyond the scope of this paper and left for future works.

Acknowledgments

This work is supported by MEXT KAKENHI Grant Number 15H05889 (M. K.), JSPS KAKENHI Grant Number 25400248 (M. K.) and also by the World Premier International Research Center Initiative (WPI), MEXT, Japan. Y. T. is supported by a JSPS Research Fellowship for Young Scientists.

References

- [1] S. Hawking, Mon. Not. Roy. Astron. Soc. **152**, 75 (1971).
- [2] B. J. Carr and S. W. Hawking, Mon. Not. Roy. Astron. Soc. **168**, 399 (1974).
- [3] B. J. Carr, Astrophys. J. **201**, 1 (1975). doi:10.1086/153853
- [4] K. Griest, A. M. Cieplak and M. J. Lehner, Phys. Rev. Lett. **111**, no. 18, 181302 (2013).
- [5] F. Capela, M. Pshirkov and P. Tinyakov, Phys. Rev. D **87**, no. 12, 123524 (2013) [arXiv:1301.4984 [astro-ph.CO]].
- [6] P. Pani and A. Loeb, JCAP **1406**, 026 (2014) doi:10.1088/1475-7516/2014/06/026 [arXiv:1401.3025 [astro-ph.CO]].
- [7] F. Capela, M. Pshirkov and P. Tinyakov, arXiv:1402.4671 [astro-ph.CO].
- [8] G. Defillon, E. Granet, P. Tinyakov and M. H. G. Tytgat, Phys. Rev. D **90**, no. 10, 103522 (2014) doi:10.1103/PhysRevD.90.103522 [arXiv:1409.0469 [gr-qc]].
- [9] J. Kormendy and D. Richstone, Ann. Rev. Astron. Astrophys. **33**, 581 (1995). doi:10.1146/annurev.aa.33.090195.003053
- [10] X. Fan *et al.* [SDSS Collaboration], Astron. J. **122**, 2833 (2001) doi:10.1086/324111 [astro-ph/0108063].
- [11] D. J. Mortlock *et al.*, Nature **474**, 616 (2011) doi:10.1038/nature10159 [arXiv:1106.6088 [astro-ph.CO]].
- [12] R. Bean and J. Magueijo, Phys. Rev. D **66**, 063505 (2002) [astro-ph/0204486].
- [13] M. Kawasaki, N. Sugiyama and T. Yanagida, Phys. Rev. D **57**, 6050 (1998) [hep-ph/9710259]. M. Kawasaki and T. Yanagida, Phys. Rev. D **59**, 043512 (1999) [hep-ph/9807544].
- [14] J. Yokoyama, Phys. Rev. D **58**, 083510 (1998) [astro-ph/9802357].
- [15] T. Kawaguchi, M. Kawasaki, T. Takayama, M. Yamaguchi and J. Yokoyama, Mon. Not. Roy. Astron. Soc. **388**, 1426 (2008) [arXiv:0711.3886 [astro-ph]].

- [16] P. H. Frampton, M. Kawasaki, F. Takahashi and T. T. Yanagida, JCAP **1004**, 023 (2010) [arXiv:1001.2308 [hep-ph]].
- [17] K. Kohri, C. M. Lin and T. Matsuda, Phys. Rev. D **87**, no. 10, 103527 (2013) doi:10.1103/PhysRevD.87.103527 [arXiv:1211.2371 [hep-ph]].
- [18] K. Kohri, D. H. Lyth and A. Melchiorri, JCAP **0804**, 038 (2008) [arXiv:0711.5006 [hep-ph]].
- [19] M. Drees and E. Erfani, JCAP **1104**, 005 (2011) [arXiv:1102.2340 [hep-ph]].
M. Drees and E. Erfani, JCAP **1201**, 035 (2012) [arXiv:1110.6052 [astro-ph.CO]].
- [20] M. Kawasaki, N. Kitajima and T. T. Yanagida, Phys. Rev. D **87**, no. 6, 063519 (2013) [arXiv:1207.2550 [hep-ph]].
- [21] E. Bugaev and P. Klimai, Phys. Rev. D **88**, no. 2, 023521 (2013) doi:10.1103/PhysRevD.88.023521 [arXiv:1212.6529 [astro-ph.CO]].
- [22] A. Linde, S. Mooij and E. Pajer, Phys. Rev. D **87**, no. 10, 103506 (2013) doi:10.1103/PhysRevD.87.103506 [arXiv:1212.1693 [hep-th]].
- [23] E. Bugaev and P. Klimai, Phys. Rev. D **90**, no. 10, 103501 (2014) doi:10.1103/PhysRevD.90.103501 [arXiv:1312.7435 [astro-ph.CO]].
- [24] A. D. Linde, Phys. Rev. D **49**, 748 (1994) [astro-ph/9307002].
- [25] G. R. Dvali, Q. Shafi and R. K. Schaefer, Phys. Rev. Lett. **73**, 1886 (1994) [hep-ph/9406319].
- [26] W. Buchmuller, L. Covi and D. Delepine, Phys. Lett. B **491**, 183 (2000) [hep-ph/0006168].
W. Buchmuller, V. Domcke and K. Schmitz, Nucl. Phys. B **862**, 587 (2012) [arXiv:1202.6679 [hep-ph]].
W. Buchmuller, V. Domcke, K. Kamada and K. Schmitz, JCAP **1407**, 054 (2014) [arXiv:1404.1832 [hep-ph]].
- [27] P. A. R. Ade *et al.* [Planck Collaboration], arXiv:1502.01589 [astro-ph.CO].
P. A. R. Ade *et al.* [Planck Collaboration], arXiv:1502.02114 [astro-ph.CO].
- [28] S. Clesse, Phys. Rev. D **83**, 063518 (2011) [arXiv:1006.4522 [gr-qc]].
- [29] H. Kodama, K. Kohri and K. Nakayama, Prog. Theor. Phys. **126**, 331 (2011) doi:10.1143/PTP.126.331 [arXiv:1102.5612 [astro-ph.CO]].
- [30] D. Mulryne, S. Orani and A. Rajantie, Phys. Rev. D **84**, 123527 (2011) doi:10.1103/PhysRevD.84.123527 [arXiv:1107.4739 [hep-th]].
- [31] S. Clesse and B. Garbrecht, Phys. Rev. D **86**, 023525 (2012) doi:10.1103/PhysRevD.86.023525 [arXiv:1204.3540 [hep-ph]].
- [32] S. Clesse, B. Garbrecht and Y. Zhu, Phys. Rev. D **89**, no. 6, 063519 (2014) doi:10.1103/PhysRevD.89.063519 [arXiv:1304.7042 [astro-ph.CO]].
- [33] J. Garcia-Bellido, A. D. Linde and D. Wands, Phys. Rev. D **54**, 6040 (1996) [astro-ph/9605094].
- [34] D. H. Lyth, JCAP **1107**, 035 (2011) [arXiv:1012.4617 [astro-ph.CO]].
D. H. Lyth, JCAP **1205**, 022 (2012) [arXiv:1201.4312 [astro-ph.CO]].
- [35] E. Bugaev and P. Klimai, JCAP **1111**, 028 (2011) [arXiv:1107.3754 [astro-ph.CO]].
E. Bugaev and P. Klimai, Phys. Rev. D **85**, 103504 (2012) [arXiv:1112.5601 [astro-ph.CO]].
- [36] A. H. Guth and E. I. Sfakianakis, arXiv:1210.8128 [astro-ph.CO].
- [37] I. F. Halpern, M. P. Hertzberg, M. A. Joss and E. I. Sfakianakis, Phys. Lett. B **748**, 132 (2015) doi:10.1016/j.physletb.2015.06.076 [arXiv:1410.1878 [astro-ph.CO]].
- [38] S. Clesse and J. Garcia-Bellido, Phys. Rev. D **92**, no. 2, 023524 (2015) [arXiv:1501.07565 [astro-ph.CO]].

- [39] J. Martin and V. Vennin, *Phys. Rev. D* **85**, 043525 (2012) doi:10.1103/PhysRevD.85.043525 [arXiv:1110.2070 [astro-ph.CO]].
- [40] L. Perreault Levasseur, V. Vennin and R. Brandenberger, *Phys. Rev. D* **88**, 083538 (2013) doi:10.1103/PhysRevD.88.083538 [arXiv:1307.2575].
- [41] T. Fujita, M. Kawasaki, Y. Tada and T. Takesako, *JCAP* **1312**, 036 (2013) [arXiv:1308.4754 [astro-ph.CO]].
- [42] T. Fujita, M. Kawasaki and Y. Tada, *JCAP* **1410**, no. 10, 030 (2014) [arXiv:1405.2187 [astro-ph.CO]].
- [43] V. Vennin and A. A. Starobinsky, *Eur. Phys. J. C* **75**, 413 (2015) doi:10.1140/epjc/s10052-015-3643-y [arXiv:1506.04732 [hep-th]].
- [44] A. A. Starobinsky, *Lect. Notes Phys.* **246**, 107 (1986). doi:10.1007/3-540-16452-9_6
- [45] Y. Nambu and M. Sasaki, *Phys. Lett. B* **205**, 441 (1988). doi:10.1016/0370-2693(88)90974-4
Y. Nambu and M. Sasaki, *Phys. Lett. B* **219**, 240 (1989). doi:10.1016/0370-2693(89)90385-7
- [46] H. E. Kandrup, *Phys. Rev. D* **39**, 2245 (1989). doi:10.1103/PhysRevD.39.2245
- [47] K. i. Nakao, Y. Nambu and M. Sasaki, *Prog. Theor. Phys.* **80**, 1041 (1988). doi:10.1143/PTP.80.1041
Y. Nambu, *Prog. Theor. Phys.* **81**, 1037 (1989). doi:10.1143/PTP.81.1037
- [48] S. Mollerach, S. Matarrese, A. Ortolan and F. Lucchin, *Phys. Rev. D* **44**, 1670 (1991). doi:10.1103/PhysRevD.44.1670
- [49] A. D. Linde, D. A. Linde and A. Mezhlumian, *Phys. Rev. D* **49**, 1783 (1994) doi:10.1103/PhysRevD.49.1783 [gr-qc/9306035].
- [50] A. A. Starobinsky and J. Yokoyama, *Phys. Rev. D* **50**, 6357 (1994) doi:10.1103/PhysRevD.50.6357 [astro-ph/9407016].
- [51] A. A. Starobinsky, *JETP Lett.* **42**, 152 (1985) [*Pisma Zh. Eksp. Teor. Fiz.* **42**, 124 (1985)].
- [52] D. S. Salopek and J. R. Bond, *Phys. Rev. D* **42**, 3936 (1990). doi:10.1103/PhysRevD.42.3936
- [53] M. Sasaki and E. D. Stewart, *Prog. Theor. Phys.* **95**, 71 (1996) doi:10.1143/PTP.95.71 [astro-ph/9507001].
- [54] M. Sasaki and T. Tanaka, *Prog. Theor. Phys.* **99**, 763 (1998) doi:10.1143/PTP.99.763 [gr-qc/9801017].
- [55] D. H. Lyth, K. A. Malik and M. Sasaki, *JCAP* **0505**, 004 (2005) doi:10.1088/1475-7516/2005/05/004 [astro-ph/0411220].
- [56] M. Morikawa, *Phys. Rev. D* **42**, 1027 (1990). doi:10.1103/PhysRevD.42.1027
- [57] W. H. Press and P. Schechter, *Astrophys. J.* **187**, 425 (1974). doi:10.1086/152650
- [58] M. W. Choptuik, *Phys. Rev. Lett.* **70**, 9 (1993). doi:10.1103/PhysRevLett.70.9
- [59] J. C. Niemeyer and K. Jedamzik, *Phys. Rev. Lett.* **80**, 5481 (1998) doi:10.1103/PhysRevLett.80.5481 [astro-ph/9709072].
- [60] F. Kuhnel, C. Rampf and M. Sandstad, arXiv:1512.00488 [astro-ph.CO].
- [61] S. Young, C. T. Byrnes and M. Sasaki, *JCAP* **1407**, 045 (2014) [arXiv:1405.7023 [gr-qc]].
- [62] T. Harada, C. M. Yoo and K. Kohri, *Phys. Rev. D* **88**, no. 8, 084051 (2013) [*Phys. Rev. D* **89**, no. 2, 029903 (2014)] [arXiv:1309.4201 [astro-ph.CO]].
- [63] B. J. Carr, K. Kohri, Y. Sendouda and J. Yokoyama, *Phys. Rev. D* **81**, 104019 (2010) [arXiv:0912.5297 [astro-ph.CO]].

- [64] D. Jeong, “Cosmology with high ($z > 1$) redshift galaxy surveys,” Diss. University of Texas, 2010.